Supporting Information

Growth of SiC whiskers onto carbonizing coir fibers by using silicon slurry waste

Yue Cao, Daoping Xiang *, Hui Li, Rong Ren, Zhiheng Xing

State Key Laboratory of Marine Resource Utilization in South China Sea, Hainan University, No. 58 People's Road, Meilan District, Haikou 570228, China.

*Corresponding author: Daoping Xiang, E-mail: dpxiang@hainu.edu.cn

Total number of pages: 9

Total number of figures: 13

S1 Experimental Section

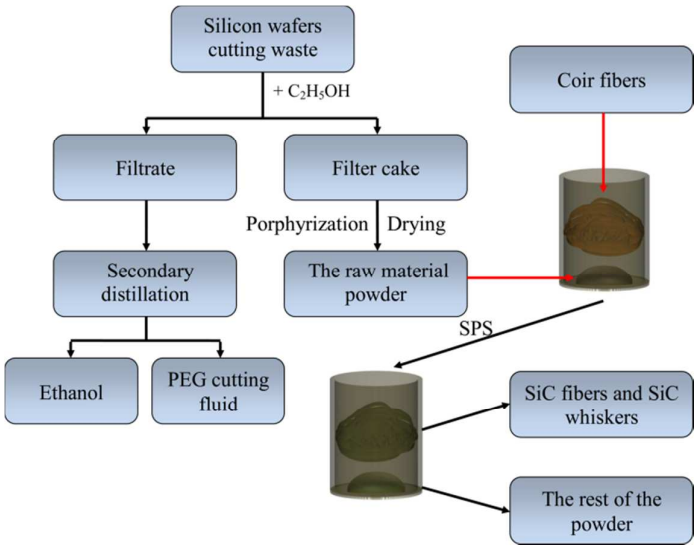

Figure S1. Flowchart of experiment.

S2 Characterization of raw materials

S2.1 Raw material powders

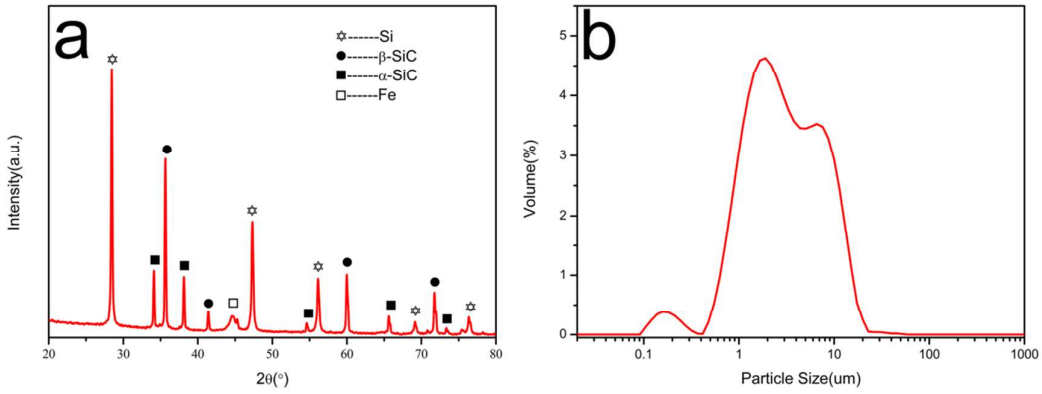

Figure S2. Raw material powders: (a) XRD pattern and (b) particle size distribution curve.

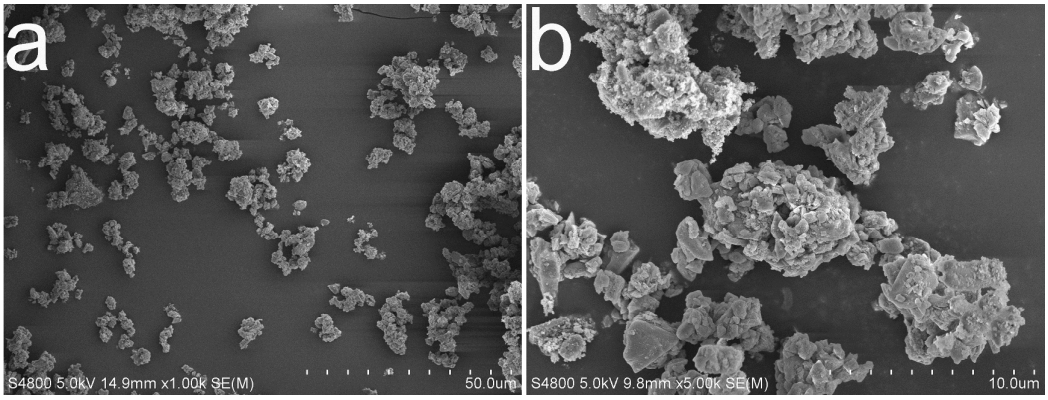

Figure S3. SEM images of raw material powders.

S2.2 Coir fibers

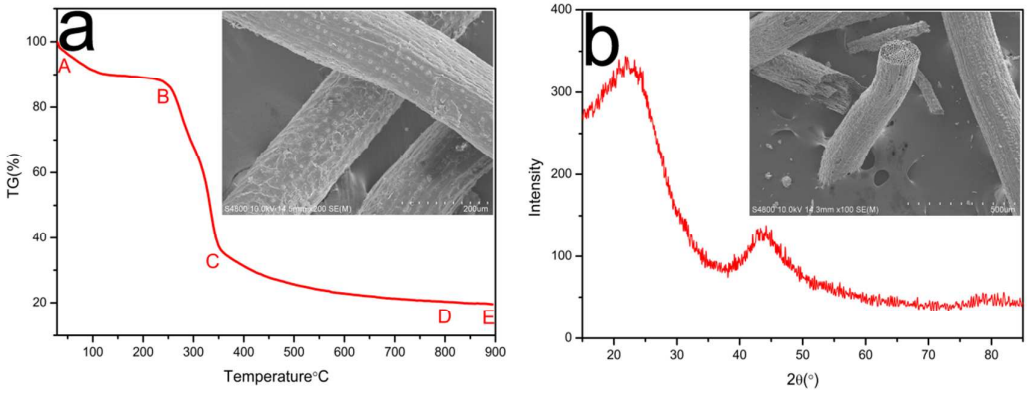

Figure S4. (a) TG curve of coir fibers (insets: SEM image) and (b) XRD pattern of carbonizing coir fibers at 1100 °C (insets: SEM image).

S2.3 Recycled PEG cutting fluid

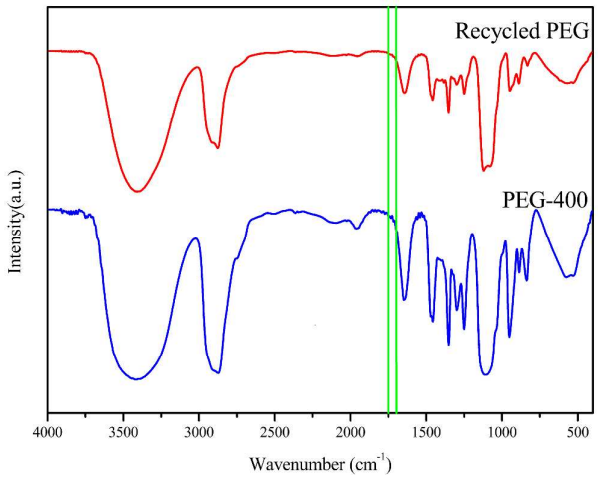

Figure S5. IR spectra of recycled PEG cutting fluid and PEG-400.

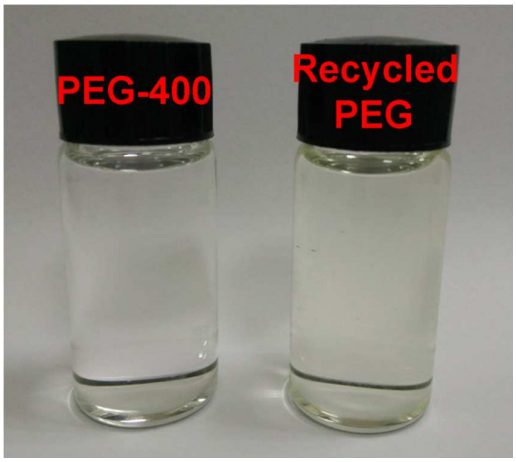

Figure S6. The photo of PEG-400 and recycled PEG cutting fluid.

When PEG is oxidized, its hydroxyl groups are easily oxidized to carbonyl groups, and the absorption peaks of carbonyl groups in IR spectra are more obvious. Therefore, to verify whether or not PEG has oxidized, it is only necessary to observe whether or not the carbonyl absorption peak exists. Characteristic peaks of carbonyl groups are located at 1700–1750 cm^{-1}. It can be seen from Figure S5 that the PEG cutting fluid recycled by two-step distillation has no oxidation reaction. Figure S6 shows that the macro chroma and macro turbidity of the recycled PEG cutting fluid had no obvious changes compared to PEG-400.

S3 The residual powders

S3.1 Phase of the residual powders

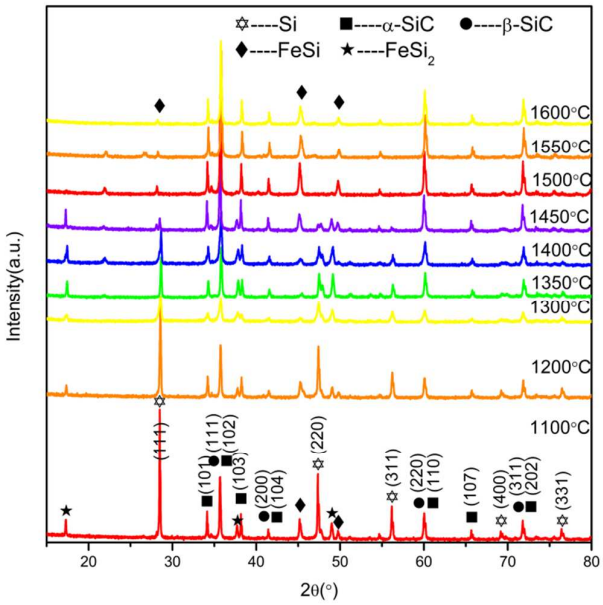

Figure S7. XRD patterns of the residual powders obtained at different temperatures.

S3.2 The K value method

In this study, the mass ratios of Si/α-SiC and Si/β-SiC ($X_{Si}/X_{\alpha\text{-}SiC}$ and $X_{Si}/X_{\beta\text{-}SiC}$) can be calculated according to the K value method as per Eq. (3)

$$\frac{X_j}{X_i} = \frac{I_j}{I_i} \times \frac{K_i}{K_j} \quad (3)$$

Among them, the K values of Si (JCPDS Card No. 75-0590), α-SiC (JCPDS Card No. 74-1302) and β-SiC (JCPDS Card No. 75-0254) were 4.55, 1.32 and 3.53, respectively. Since both the first and second strongest diffraction peaks of α-SiC and β-SiC coincide in the XRD pattern, the third strongest peaks (α-SiC (101) and β-SiC (311)) are used to calculate the $X_{Si}/X_{\alpha\text{-}SiC}$ and $X_{Si}/X_{\beta\text{-}SiC}$ values.

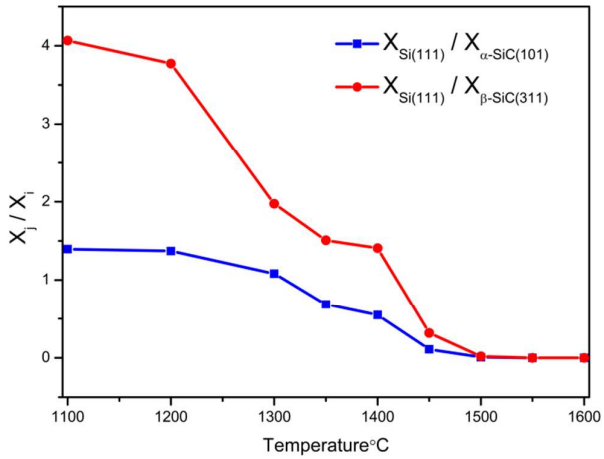

Figure S8. Si content ratio chart of the residual powders obtained at different temperatures.

S3.3 particle size of the residual powders

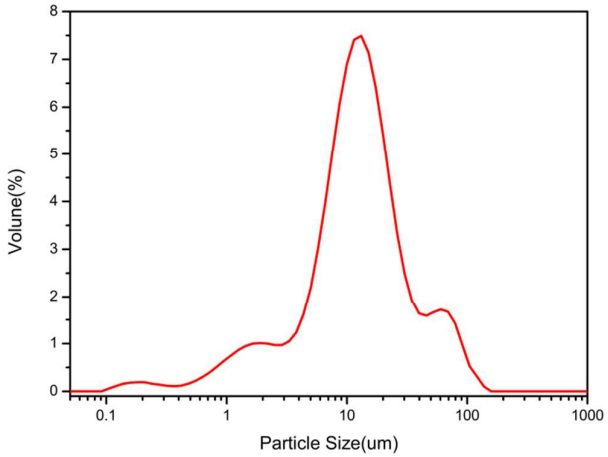

Figure S9. Particle size distribution curve of the residual powders obtained at 1500 °C.

S4. SiC whiskers

S4.1 XRD analysis

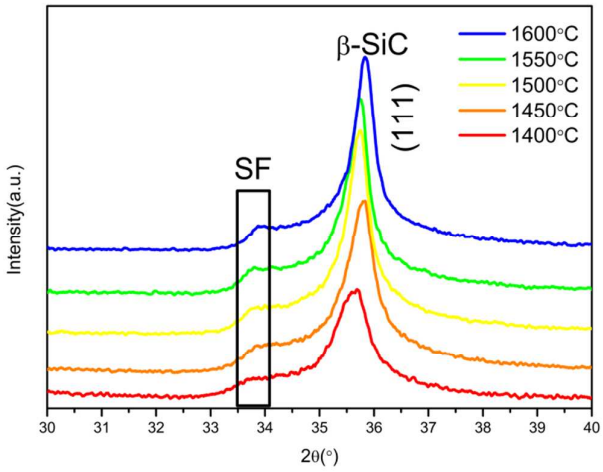

Figure S10. Local XRD patterns of the SiC whiskers and fiber substrates at different preparation temperatures.

S4.2 Growth mechanisms

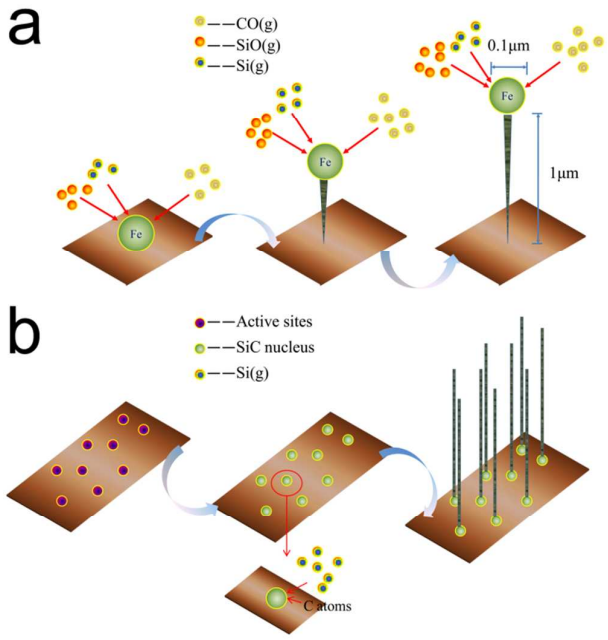

Figure S11. SiC whisker growth mechanism. (a) VLS and (b) VS growth mechanisms.

S4.3 Thermodynamic feasibility analysis

Thermodynamic calculations over a wide temperature range (1000–1600 °C) for these free energy changes and enthalpy changes of the reactions were carried out using the data obtained from HSC Chemistry thermochemical software (HSC Chemistry 6). Figure S12 shows the temperature dependence of Gibbs free energy reflected in reactions (4)–(10) in the temperature range (1000–1600 °C) at atmospheric pressure. Clearly, based on the analysis of both free energy and enthalpy, reactions (6)–(10) can proceed spontaneously in this temperature range at atmospheric pressure. According to Eq. (S1), the Gibbs free energy change formula (Eqs. (S2)–(S3)) of reactions (4)–(5) can be derived. In this experiment, coir fibers are pyrolyzed to produce a large amount of CO, which causes high CO gas pressure in the small volume mould. Note that the gas phase of SiO originated from reactions (4) was metastable, which was helpful for the occurrence of reaction (5). [36] At 1100–1300 °C, under conditions of CO and SiO vapor saturation, reaction (5) can be carried out. [42] Moreover, catalytic iron promoted the reaction in this experiment. Thermodynamic analysis shows that these reactions are feasible.

$$\Delta G = \Delta G^0 + RTlnQ \quad (S1)$$

$$\Delta G_{(4)} = \Delta G^0_{(4)} + RTln\frac{P_{SiO}}{P_{CO}} \quad (S2)$$

$$\Delta G_{(5)} = \Delta G^0_{(5)} + RTln\frac{(P_{CO_2})^2}{(P_{CO})^3(P_{SiO})} \quad (S3)$$

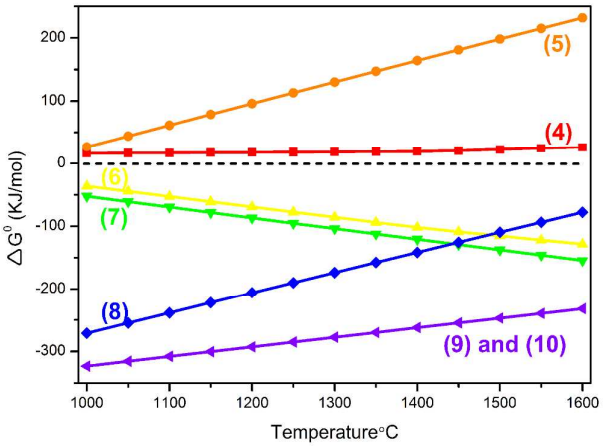

Figure S12. Gibbs free energy changes for reactions (4)–(10) at atmospheric pressure.

S4.2 TEM analysis

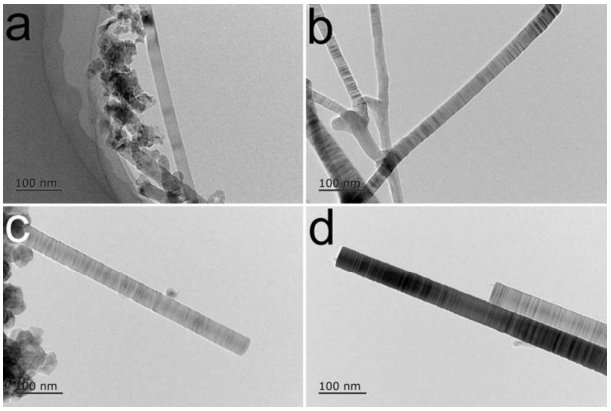

Figure S13. TEM images of SiC whiskers prepared at 1500 °C.